An Adaptive Rational Filter for Interpretation of Spectrometric Data

Michal P. Wiśniewski, Roman Z. Morawski, *Senior Member, IEEE*, and Andrzej Barwicz, *Member, IEEE*

***Abstract*—The computer-based interpretation of spectrometric data is of great importance for applications of various kinds of spectroscopy in science, biomedical engineering, environmental engineering, and industry. It is based on the use of algorithms of (generalized) deconvolution for correcting spectrometric data, i.e., compensating for the instrumental effects and natural bandwidth effects distorting those data. Among many sophisticated methods currently used for this purpose, no one method is able to properly deal with the irregularities in the data such as the variable shape of peaks of which the interpreted spectrum is composed. In this paper, a flexible and efficient algorithm of generalized deconvolution is proposed, *viz*. an adaptive rational filter. It is proven to satisfactorily solve this problem by recursive adaptation of its parameters to the widths of the consecutive peaks of which the interpreted spectrum is composed, as well as to the relative distances between peaks along the wavelength axis.**

I. Introduction

THE COMPUTER-BASED interpretation of spectrometric data usually involves the use of algorithms of deconvolution or algorithms of generalized deconvolution (being an operation not strictly inverse to convolution). These algorithms are of great importance for applications of various kinds of spectroscopy in science, biomedical engineering, environmental engineering, and industry. An extensive review of relevant publications, which had appeared until 1997, may be found in [1]. Let us mention only a few of the more recent applications where the algorithms of (generalized) deconvolution are used:

- identification of pesticides in mixtures by means of UV-range spectroscopy [2];
- identification of contaminants and chemical modifications of biomacromolecules by means of an electrospray ionization technique and mass spectroscopy [3];
- analysis of particulate mixtures on Earth and Mars by means of IR-range telespectroscopy [4];
- analysis of chemical composition and state surface constituents of pyritre, marcasite and arsenopyrite by means of X-ray photoelectron spectroscopy [5];
- bone marrow inspection by means of NMR spectrometry [6].

Manuscript received January 6, 2002; revised November 22, 2002. This work was supported in part by the Natural Sciences and Engineering Research Council of Canada, the Government of Quebec, and the State Committee for Scientific Research, Poland under Grant 8 T10C 025 11.

M. P. Wiśniewski and A. Barwicz are with the Department of Electrical Engineering, University of Québec, Trois-Rivières, QC, G9A 5H7 Canada (e-mail: Michal_Wiśniewski@uqtr.uquebec.ca; Andrzej_Barwicz@uqtr.uquebec.ca).

R. Z. Morawski is with the Faculty of Electronics and Information Technology, Institute of Radioelectronics, Warsaw University of Technology, Warsaw, Poland (e-mail: R.Morawski@ire.pw.edu.pl).

Digital Object Identifier 10.1109/TIM.2003.809066

Among many algorithms of (generalized) deconvolution currently used for correcting spectrometric data (i.e., compensating for the instrumental effects and natural bandwidth effects distorting those data), no one algorithm is able to properly deal with the irregularities in the data such as the variable shape of peaks of which the interpreted spectrum is composed. In this paper, a flexible and efficient algorithm of generalized deconvolution is proposed, *viz*. an adaptive rational filter (ARF), which is proven to satisfactorily solve this problem. A general methodology for spectrometric data interpretation is outlined in Section II, the ARF is developed in Section III, and the methodology for its investigation in Section IV. The results of tests, carried out using both synthetic and real-world data, are summarized in Section V, while in Section VI, some key conclusions are formulated concerning the practical applicability of the proposed method of spectrometric data interpretation. Throughout the paper, the following notation is used:

λ	wavelength, $\lambda \in [\lambda_{\min}, \lambda_{\max}]$;
$x^{\mathrm{Tr}}(\lambda) \in [0, 1]$	transmittance spectrum;
$x^{\mathrm{Ab}}(\lambda) = -\log_{10}[x^{\mathrm{Tr}}(\lambda)] \in [0, +\infty)$	absorbance spectrum;
$s^{\mathrm{Ab}}(\lambda) \in [0, +\infty)$	idealized absorbance spectrum;
$\{\tilde{y}_n^{\mathrm{Tr}}\}$	transmittance-domain data;
$\{\tilde{y}_n^{\mathrm{Ab}}\} = \mathbf{A}\{\tilde{y}_n^{\mathrm{Tr}}\} \equiv \{-\log_{10}(\tilde{y}_n^{\mathrm{Tr}})\}$	absorbance-domain data;
$\{\hat{x}_n^{\mathrm{Ab}}\}$	discrete estimate of the absorbance spectrum;
$\{\hat{s}_n^{\mathrm{Ab}}\}$	discrete estimate of the idealized absorbance spectrum.

II. Interpretation of Spectrometric Data

The resolution of spectrometric analysis is limited by two independent factors:

- the instrumental imperfections of the spectrometer, which may be roughly characterized by a parameter called *spectral bandwidth* (SBW);
- the *natural bandwidth* (NBW) of the absorbing substance, which is usually characterized by the width of the normalized absorption peak at the half of its maximum.

The following set of algorithms was suggested in [7] to reduce the effect of both factors on the result of spectrometric analysis:

0018-9456/03$17.00 © 2003 IEEE

- the rational filter, as proposed and studied in [8] and [9], to remove the instrumental effect from the data acquired by means of a spectrometer;
- the spline-based Kalman filter with a positivity constraint, as proposed and studied in [10], to estimate the parameters of the spectrum, i.e., positions and magnitudes of the peaks of which it is composed;
- a recursive algorithm of least-squares estimation, to correct the estimates of the magnitudes of peaks.

The use of the first of the above algorithms is based on the assumption that the instrumental effect may be adequately modeled by [1]

$$\{\tilde{y}_n^{\mathrm{Tr}}\} = \left\{g_{\mathrm{SBW}}(\lambda) * x^{\mathrm{Tr}}(\lambda)|_{\lambda=\lambda_n}\right\} + \{\eta_n\} \tag{1}$$

where $*$ denotes the convolution operator, λ is wavelength, $\lambda_n = \lambda_{\min} + (n-1)(\lambda_{\max} - \lambda_{\min})/(N-1)$ for $n = 1, \ldots, N$, $g_{\mathrm{SBW}}(\lambda)$ is the optical response function modeling the effect of the spectral bandwidth, $x^{\mathrm{Tr}}(\lambda)$ is the transmittance of the analyzed sample, $\{\tilde{y}_n^{\mathrm{Tr}}\}$ is the result of its measurement, i.e., the spectrometric data, and $\{\eta_n\}$ are realizations of zero-mean random variables with the variance σ_η^2, modeling the errors corrupting the spectrometric data. The result of correction of the data $\{\tilde{y}_n^{\mathrm{Tr}}\}$, obtained by means of the rational filter and denoted with $\{\hat{x}_n^{\mathrm{Tr}}\}$, is converted into absorbance

$$\{\hat{x}_n^{\mathrm{Ab}}\} = \mathbf{A}\{\hat{x}_n^{\mathrm{Tr}}\} \equiv \{-\log_{10}(\hat{x}_n^{\mathrm{Tr}})\} \tag{2}$$

and then the effect of NBW is reduced using the spline-based Kalman filter derived under an assumption that

$$\{\hat{x}_n^{\mathrm{Ab}}\} = \left\{g_{\mathrm{NBW}}(\lambda) * s^{\mathrm{Ab}}(\lambda)|_{\lambda=\lambda_n}\right\} \tag{3}$$

where $g_{\mathrm{NBW}}(\lambda)$ is the optical response function modeling the effect of the natural bandwidth of the analyzed sample, and $s^{\mathrm{Ab}}(\lambda)$ is its idealized (hypothetical) spectrum as it would appear in the absence of this effect. The latter spectrum is assumed to have the form

$$s^{\mathrm{Ab}}(\lambda) \equiv s^{\mathrm{Ab}}(\lambda; \mathbf{l}, \mathbf{a}) = \sum_{k=1}^{K} a_k \delta(\lambda - l_k) \tag{4}$$

where K is the number of peaks, $\mathbf{l} = [l_1 \cdots l_K]^T$ is the vector of the positions of peaks, $\mathbf{a} = [a_1 \cdots a_K]^T$ is the vector of the magnitudes of peaks, and $\delta(\cdot)$ is the Dirac delta distribution. A discrete estimate $\{\hat{s}_n^{\mathrm{Ab}}\}$ of $s^{\mathrm{Ab}}(\lambda)$, obtained by means of the spline-based Kalman filter, is used for computing some initial estimates of the positions and magnitudes of peaks. They could be next corrected by means of an iterative algorithm described in [12], but for the sake of simplicity an algorithm, formally similar to the Kalman filter, has been chosen (exclusively for correction of the estimates of the magnitudes). This is a recursive least-squares algorithm improving the fit of the model of absorption

$$\left\{g_{\mathrm{NBW}}(\lambda) * s^{\mathrm{Ab}}(\lambda; \hat{\mathbf{l}}; \mathbf{a})|_{\lambda=\lambda_n}\right\} = \left\{\sum_{k=1}^{K} a_k g_{\mathrm{NBW}}(\lambda_n - \hat{l}_k)\right\} \tag{5}$$

to its estimate $\{\hat{x}_n^{\mathrm{Ab}}\}$ using an estimate $\hat{\mathbf{l}}$ of the vector of positions of peaks $\mathbf{l}$. It has the form

$$\hat{\mathbf{a}}^{(n+1)} = \hat{\mathbf{a}}^{(n)} + \mu \mathbf{g}_n \left(\hat{x}_n^{\mathrm{Ab}} - \mathbf{g}_n^T \hat{\mathbf{a}}^{(n)}\right) \quad \text{for } n = 1, \ldots, N \tag{6}$$

where $\mu \in [0, 1]$ is a relaxation coefficient, and

$$\mathbf{g}_n = \left[g_{\mathrm{NBW}}\left(\lambda_n - \hat{l}_1\right) \cdots g_{\mathrm{NBW}}\left(\lambda_n - \hat{l}_K\right)\right]^T. \tag{7}$$

The satisfactory performance of the above-described set of algorithms has been demonstrated on many examples of spectrometric data representative of the spectra composed of peaks whose shapes are considered to be relatively uniform. It has been noticed, however, that they may fail if the data to be interpreted represent the spectrum composed of peaks significantly differing in the height-to-width ratio: a larger peak may be then identified as a composition of several narrow peaks. This observation underlies the idea of an ARF, proposed in this paper, to replace the Kalman filter in the above-described set of algorithms for interpretation of spectrometric data.

III. Proposed ARF

The jth-order rational filter (RF) is defined recursively [8]

$$\mathrm{RF}_j[\{\tilde{y}_n\}] = \begin{cases} \{\tilde{y}_n\}, & \text{for } j = 0 \\ \dfrac{\{\tilde{y}_n\} \cdot \mathrm{RF}_{j-1}[\{\tilde{y}_n\}]}{\{h_{K,n}\} * \mathrm{RF}_{j-1}[\{\tilde{y}_n\}]}, & \text{for } j > 0 \end{cases} \tag{8}$$

where $\{h_{j,l}\}$ are the filter parameters satisfying the following constraints:

$$h_{j,l} \geq 0, \qquad \text{for } l = -L, \ldots, L \tag{9}$$

$$\sum_{l=-L}^{L} h_{j,l} = 1, \qquad \sum_{l=-L}^{L} k \cdot h_{j,l} = 0. \tag{10}$$

When this filter is applied for removing the instrumental effect

$$\{\hat{x}_n^{\mathrm{Tr}}\} = \mathbf{R}\left[\{\tilde{y}_n^{\mathrm{Tr}}\}; \mathbf{p}_{\mathbf{R}}^{RF}\right] \tag{11}$$

then its parameters

$$\mathbf{p}_{\mathbf{R}}^{RF} = \left[h_{1,-L}^{RF} \cdots h_{1,L}^{RF} \cdots h_{j,-L}^{RF} \cdots h_{j,L}^{RF}\right]^T \tag{12}$$

are estimated according to the formula

$$\hat{\mathbf{p}}_{\mathbf{R}}^{RF} = \arg_{\mathbf{p}} \inf \left\{ \left\| \mathbf{A} \circ \mathbf{R}\left[\{y_n^{\mathrm{Tr,cal}}\}; \mathbf{p}\right] - \mathbf{A}\{x_n^{\mathrm{Tr,cal}}\}\right\|_2^2 | \mathbf{p} \in \mathbf{p}\right\} \tag{13}$$

using the calibration data, $\{x_n^{\mathrm{Tr,cal}}\}$ and $\{y_n^{\mathrm{Tr,cal}}\}$, and the set of constraints $\mathbf{P}$ defined by (9) and (10).

The parameters of the proposed ARF $\mathbf{p}_{\mathbf{R}}^{\mathrm{ARF}}$ depend on the width parameters of the peaks to be processed $\boldsymbol{\sigma} = [\sigma_1 \cdots \sigma_K]^T$, and on the distances between consecutive peaks $\boldsymbol{\Delta}\mathbf{l} = [\Delta l_2 \cdots \Delta l_K]^T$, where $\Delta l_k = l_k - l_{k-1}$ for $k = 2, \ldots, K$. More precisely, the parameters of the ARF depend on σ_k, Δl_k and Δl_{k+1} when the data corresponding to the kth peak are processed.

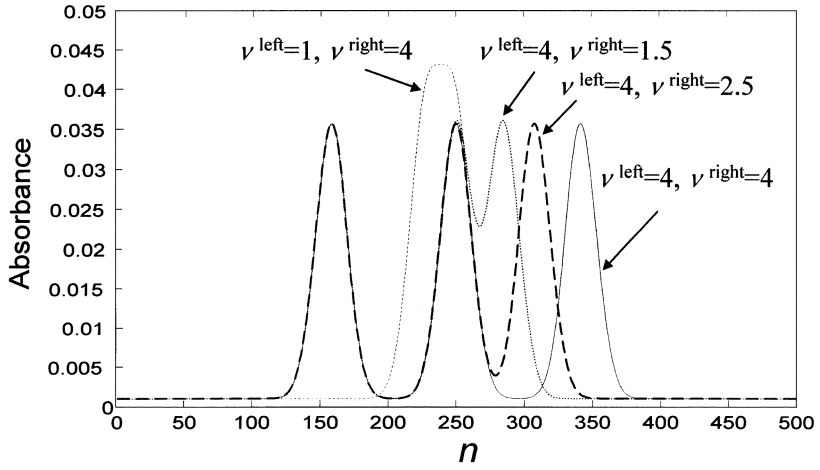

Fig. 1. Calibration data used for estimation of the ARF parameters corresponding to $\sigma = 5$.

The design of the ARF is based on the assumption that the spectral peaks may be approximated using the Gauss functions $\text{Gauss}(\lambda - l_k; \sigma_k^2)$, where

$$\text{Gauss}(\lambda; \sigma^2) = \frac{1}{\sqrt{2\pi}\sigma} \exp\left(-\frac{\lambda^2}{2\sigma^2}\right). \tag{14}$$

If the ARF is designed for correcting the NBW effect of the analyzed substance

$$\left\{\hat{s}_n^{\text{Ab}}\right\} = \mathbf{R}\left[\left\{\hat{x}_n^{\text{Ab}}\right\}; \mathbf{p}_{\mathbf{R}}^{\text{ARF}}\right] \tag{15}$$

then its parameters

$$\mathbf{p}_{\mathbf{R}}^{\text{ARF}} = \left[h_{1,-L}^{\text{ARF}} \cdots h_{1,L}^{\text{ARF}} \cdots h_{j,-L}^{\text{ARF}} \cdots h_{j,L}^{\text{ARF}}\right]^T \tag{16}$$

are estimated according to the formula

$$\hat{\mathbf{p}}_{\mathbf{R}}^{\text{ARF}} = \arg_{\mathbf{p}} \inf\left\{ \left\|\mathbf{R}\left[\left\{x_n^{\text{Ab, cal}}\right\}; \mathbf{p}\right] - \left\{s_n^{\text{Ab, cal}}\right\}\right\|_2^2 \middle| \mathbf{p} \in \mathbf{P}\right\} \tag{17}$$

using the calibration data, $\{s_n^{\text{Ab, cal}}\}$ and $\{x_n^{\text{Ab, cal}}\}$, and the set of constraints **P** defined by (9) and (10).

The data for calibration, i.e., for estimation of the ARF parameters according to (17), are generated according to the formulas

$$s_n^{\text{Ab, cal}} = \begin{cases} 1, & \text{for } n - 250 = -\nu^{\text{left}} \dfrac{\sigma}{\Delta\lambda},\ 0,\ \nu^{\text{right}} \dfrac{\sigma}{\Delta\lambda} \\ 0, & \text{otherwise} \end{cases} \tag{18}$$

$$\begin{aligned} x_n^{\text{Ab, cal}} = &\text{Gauss}\left(\lambda_n - 250\Delta\lambda + \nu^{\text{left}}\sigma; \sigma^2\right) \\ &+ \text{Gauss}\left(\lambda_n - 250\Delta\lambda; \sigma^2\right) \\ &+ \text{Gauss}\left(\lambda_n - 250\Delta\lambda - \nu^{\text{right}}\sigma; \sigma^2\right) \end{aligned} \tag{19}$$

where σ, ν^{left}, and ν^{right} are parameters of a set of the synthetic data defining the relative width and relative positions of a three-peak spectrum represented by the data. Such a parameterization of the data used for calibration makes it possible to train the ARF as to adapt it to the varying width and distribution of peaks along the wavelength axis. To get the representative collection of the ARF parameters, 576 sets of calibration data

TABLE I
SET OF ALGORITHMS FOR THE INTERPRETATION OF SPECTROMETRIC DATA

#	Algorithms
1	$\left\{\hat{x}_n^{\text{Tr}}\right\} = \text{RF}\left(\left\{\tilde{y}_n^{\text{Tr}}\right\}, \left\{h_n^{\text{RF}}\right\}, L^{\text{RF}}\right)$
2	$\left\{\hat{x}_n^{\text{Ab}}\right\} = \text{LOG}\left(\left\{\hat{x}_n^{\text{Tr}}\right\}\right)$
3	$\breve{\mathbf{l}} = \text{PEAK\_POS}\left(\left\{\hat{x}_n^{\text{Ab}}\right\}\right) \Rightarrow \Delta\mathbf{l}$
4	$\hat{\boldsymbol{\sigma}} = \text{PEAK\_WID}\left(\left\{\hat{x}_n^{\text{Ab}}\right\}\right)$
5	$\left\{\hat{s}_n^{\text{Ab}}\right\} = \text{ARF}\left(\left\{\hat{x}_n^{\text{Ab}}\right\}, \left\{h_n^{\text{ARF}}(\hat{\boldsymbol{\sigma}}, \Delta\mathbf{l})\right\}, L^{\text{ARF}}\right)$
6	$\hat{\mathbf{l}} = \text{PEAK\_POS}\left(\left\{\hat{s}_n^{\text{Ab}}\right\}\right)$
7	$\hat{\mathbf{a}} = \text{PEAK\_MAG}\left(\left\{\hat{x}_n^{\text{Ab}}\right\}, \boldsymbol{g}_{\text{NBW}}, \hat{\mathbf{l}}, \mu, K\right)$

are generated and stored, corresponding to all possible combinations of the following values of the parameters of (18) and (19):

$$\sigma \in \{0.2,\ 1,\ 2,\ \ldots,\ 15\} \tag{20}$$

$$\nu^{\text{left}},\ \nu^{\text{right}} \in \{1,\ 1.5,\ 2,\ 2.5,\ 3,\ 4\}. \tag{21}$$

In Fig. 1, some exemplary sets of the calibration data $\{x_n^{\text{Ab, cal}}\}$ corresponding to $\sigma = 5$ are shown.

The dependence of the ARF parameters $\mathbf{p}_{\mathbf{R}}^{\text{ARF}}$ on σ, ν^{left} and ν^{right} is approximated using the polynomial cubic β-spline function in three variables [13].

- First, the sets of calibration data, corresponding to 576 triplets $\langle\sigma, \nu^{\text{left}}, \nu^{\text{right}}\rangle$, are generated.
- Next, for each set of calibration data, an estimate $\hat{\mathbf{p}}_{\mathbf{R}}^{\text{ARF}}$ is computed.
- Finally, a β-spline function

$$\mathbf{p}_{\mathbf{R}}^{\text{ARF}} = Spl\beta 3(\sigma, \nu^{\text{left}}, \nu^{\text{right}}) \tag{22}$$

is evaluated on the basis of the estimates $\hat{\mathbf{p}}_{\mathbf{R}}^{\text{ARF}}$ and corresponding triplets $\langle\sigma, \nu^{\text{left}}, \nu^{\text{right}}\rangle$.

The function defined by (22) is used for adaptation of the ARF during the processing of the sequence $\{\hat{x}_n^{\text{Ab}}\}$. The following strategy is used for this purpose.

- First, a pre-estimate $\breve{\mathbf{l}} = [\breve{l}_1 \cdots \breve{l}_K]^T$ of the positions of peaks is determined using the first and second derivative of the data $\{\hat{x}_n^{\text{Ab}}\}$ wherein the second derivative is used for

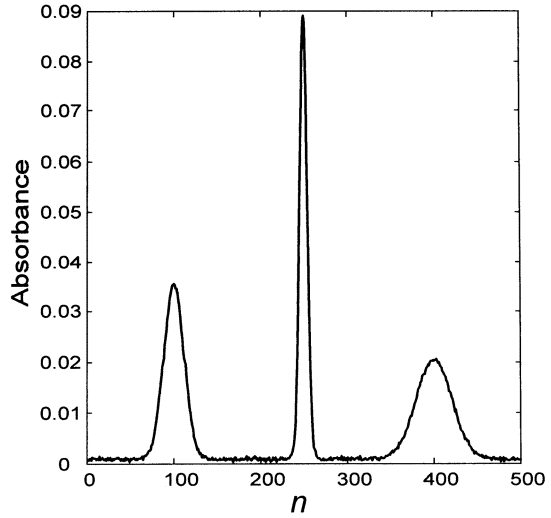

(a)

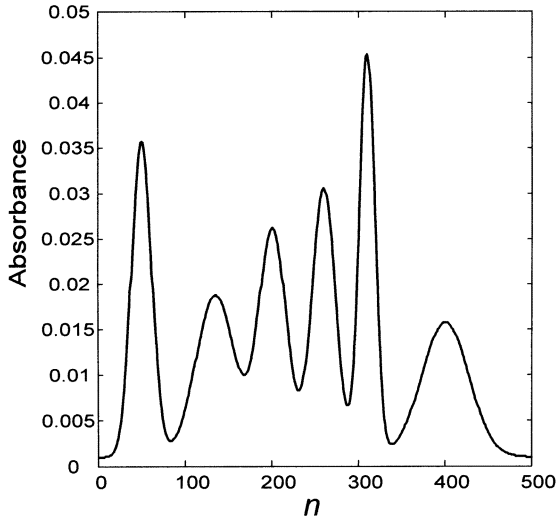

(b)

Fig. 2. Exact synthetic data used for testing the ARF.

detection of overlapping peaks, which cannot be detected by means of the first derivative.

- Next, an estimate $\hat{\boldsymbol{\sigma}} = [\hat{\sigma}_1 \cdots \hat{\sigma}_K]^T$ of the vector of width parameters is calculated on the basis of the width of peaks estimated at 75% of their heights.
- Then, the ARF parameters for every detected peak are computed according to the formulas

$$\nu_k^{\text{left}} = \begin{cases} 4, & k = 1 \\ \frac{\breve{\imath}_k - \breve{\imath}_{k-1}}{\hat{\sigma}_k}, & k > 1 \end{cases} \tag{23}$$

$$\nu_k^{\text{left}} = \begin{cases} \frac{\breve{\imath}_{k+1} - \breve{\imath}_k}{\hat{\sigma}_k}, & k < K \\ 4, & k = K \end{cases} \tag{24}$$

$$\hat{\mathbf{p}}_{\mathbf{R},\,k}^{\text{ARF}} = Spl\beta 3\left(\hat{\sigma}_k,\, \nu_k^{\text{left}},\, \nu_k^{\text{right}}\right), \quad \text{for } k = 1,\, \ldots,\, K. \tag{25}$$

- After that, the values of the ARF parameters between two consecutive peaks, k and $(k+1)$, are approximated using a parabolic β-spline function

$$\hat{\mathbf{p}}_{\mathbf{R},\,n}^{\text{ARF}} = Spl\beta 2(\lambda_n). \tag{26}$$

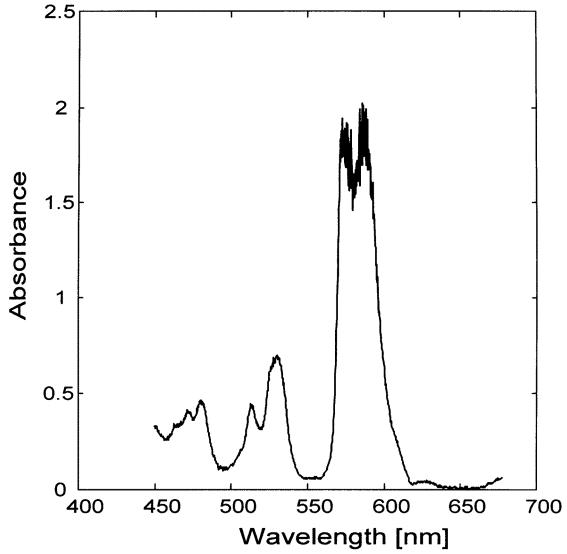

Fig. 3. Estimate of the real-world absorption spectrum of didymium (obtained by means of the algorithm RF and by means of the algorithm LOG) used for testing the ARF.

- Finally, the estimate $\hat{s}_n^{\text{Ab}}$ is calculated with the formula

$$\hat{s}_n^{\text{Ab}} = \mathbf{R}\left[\left\{\hat{x}_n^{\text{Ab}}\right\}; \mathbf{p}_{\mathbf{R},\,n}^{\text{ARF}}\right], \qquad \text{for } n = 1,\, \ldots,\, N. \tag{27}$$

The set of algorithms for the interpretation of spectrometric data, containing the ARF, is synthetically described in Table I, where RF is the rational filter for correction of instrumental imperfections, LOG is the algorithm of transmittance-to-absorbance conversion, PEAK_POS is the algorithm for estimation of peak positions, PEAK_WID is the algorithm for estimation of peak widths, and PEAK_MAG is the algorithm for estimation of peak magnitudes.

IV. Methodology for Testing the ARF

The ARF was tested using both synthetic and real-world data.

The exact synthetic data $\{x_n^{\text{Ab}}\}$, representative of some absorption spectra composed of Gaussian peaks, are shown in Fig. 2. The values of $\sigma/\Delta\lambda$ characterizing the widths of peaks in Fig. 2(a) are 23, 9, and 41; the values of $\sigma/\Delta\lambda$ for peaks in Fig. 2(b) are 23, 45, 32, 27, 18, and 54. The error-corrupted synthetic data $\{\hat{x}_n^{\text{Ab}}\}$ were produced according to the formula

$$\{\hat{x}_n^{\text{Ab}}\} = \{x_n^{\text{Ab}}\} + \{\varepsilon_n\} \tag{28}$$

where $\{\varepsilon_n\}$ are realizations of identical, independent random variables following the zero-mean normal distribution with the variance of 10^{-8}.

The real-world data, representative of the absorption spectrum of a standard sample of didymium, are shown in Fig. 3. They were acquired by means of the reference spectrometer VARIAN CARY-3 with the optical resolution of 5 nm, and processed by the algorithms #1 and #2 as defined in Table I, where L^{RF} and L^{ARF} denote the "lengths" of the RF and of the ARF, respectively. Two indicators, *viz.* the normalized root-mean-square error

$$\partial_2^l = \frac{\left\|\hat{\mathbf{l}} - \mathbf{l}\right\|_2}{\|\mathbf{l}\|_2}, \qquad \partial_2^a = \frac{\|\hat{\mathbf{a}} - \mathbf{a}\|_2}{\|\mathbf{a}\|_2} \tag{29}$$

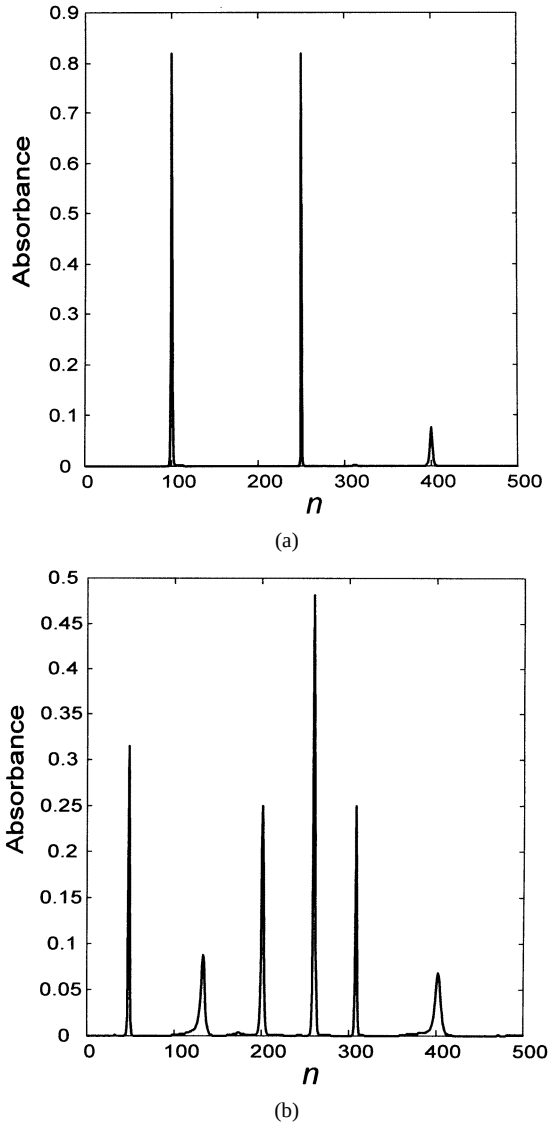

Fig. 4. Estimates $\{\hat{s}_n^{\mathrm{Ab}}\}$ of the idealized spectrum of (a) Fig. 2 (a) and (b), obtained by means of the proposed ARF.

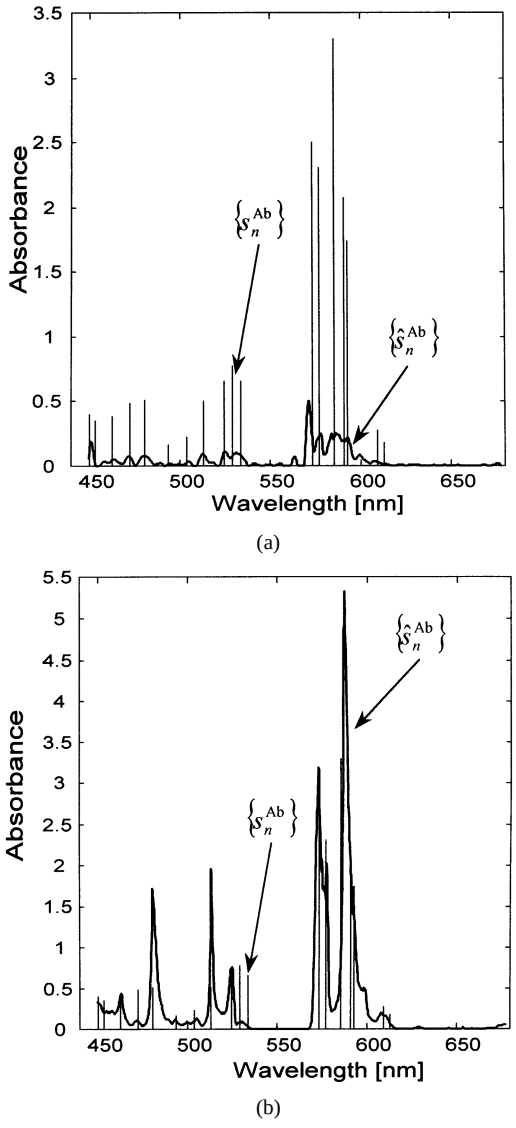

Fig. 5. Estimates of the idealized spectrum of didymium, obtained by (a) means of the currently used algorithm and by (b) means of the proposed ARF.

and the normalized maximum error

$$\partial_{\infty}^{l} = \frac{\left\|\hat{\mathbf{l}} - \mathbf{l}\right\|_{\infty}}{\|\mathbf{l}\|_{\infty}}, \qquad \partial_{\infty}^{a} = \frac{\|\hat{\mathbf{a}} - \mathbf{a}\|_{\infty}}{\|\mathbf{a}\|_{\infty}} \tag{30}$$

were used for the assessment of the ARF, i.e., of the uncertainty of estimation of the positions and of the magnitudes of peaks.

V. Results of Testing the ARF

The results of testing the ARF with the error-free synthetic data are shown in Fig. 4 (the results obtained for error-corrupted data differ only at the level of $\sim 10^{-6}$).

The results of testing the ARF with the real-world data are shown in Fig. 5. A quite striking improvement in the accuracy of estimation of the idealized spectrum is observed when the currently used algorithm based on spline approximation and Kalman filtering (SPL_KAL) [11] is replaced with the proposed ARF. Of course, it implies a corresponding improvement in the quality of the estimates of the spectrum parameters, obtained on the basis of $\{\hat{s}_n^{\mathrm{Ab}}\}$. The results of computation, obtained by means of the ARF and SPL_KAL, are systematically compared in Table II. For all the sets of data used for experimentation, the results obtained by means of the ARF are better than those obtained by means of the SPL_KAL with respect to all six criteria of comparison: the number of undetected peaks, the number of artifacts, ∂_2^l, ∂_{∞}^l, ∂_2^a, and ∂_{∞}^a. It is worth stressing that the estimates of the positions of peaks, obtained by means of the ARF, are subject to an error smaller than $\Delta\lambda$ while for the fixed-parameter RF this error may reach $2\Delta\lambda$.

The numerical complexity of the ARF is characterized in Table III by the number of floating-point operations (computed by means of the MATLAB procedure **flops**), necessary for correcting the data representative of a spectrum composed of K peaks ($K = 1, \ldots, 10$).

VI. Conclusion

The ARF, proposed in this paper, has been tested (using both synthetic and real-world data) as a means for reducing the negative impact of the natural bandwidth of an analyzed substance

TABLE II
COMPARISON OF THE RESULTS OBTAINED BY MEANS OF THE ARF AND BY MEANS OF THE SPL_KAL ALGORITHM

Data	Algorithm	Number of undetected	Number of artifacts	∂_2'	∂_∞'	∂_2^a	∂_∞^a
Synthetic data (Fig. 2a)	ARF	0	0	0	0	0.55	0.92
	SPL_KAL	0	6	0	0	0.97	1.00
Synthetic data (Fig. 2b)	ARF	0	0	0.006	0.005	0.77	0.93
	SPL_KAL	1	4	0.035	0.053	0.95	1.00
Real-world data (didymium)	ARF	1	1	0.014	0.031	0.46	0.49
	SPL_KAL	2	7	0.042	0.054	0.69	0.75

TABLE III
COMPLEXITY OF COMPUTATION

Number of peaks	Flops
1	627 213
2	729 893
3	832 573
4	935 214
5	1 037 894
6	1 140 574
7	1 243 254
8	1 346 002
9	1 448 688
10	1 551 363

on the accuracy of estimates of the positions of peaks of which the spectrum of the analyzed substance is composed. The ARF is adjusting its parameters to the shapes of the peaks during the processing of spectrometric data. Consequently, it is able to correctly interpret the data representative of spectra composed of peaks differing in the height-to-width ratio. The quantitative results obtained confirm the superiority of the ARF to the previously published algorithm based on spline approximation and Kalman filtering.

REFERENCES

[1] P. A. Jansson, Ed., *Deconvolution of Spectra and Images*. New York: Academic, 1997.

[2] F. Cuesta Sanchez, S. C. Rutan, M. D. Gil Garcia, and D. L. Massart, "Resolution of multicomponent overlapped peaks by the orthogonal projection approach, evolving factor analysis and window factor analysis," *Chemometr. Intelligent Lab. Syst.*, vol. 36, pp. 153–164, 1997.

[3] Z. Zhang and A. G. Marshall, "A universal algorithm for fast and automated charge state deconvolution of electrospray mass-to-charge ratio spectra," *J. Amer. Soc. Mass Spectrom.*, vol. 9, pp. 225–233, 1998.

[4] M. S. Ramsey and P. R. Christensen, "Mineral abundance determination: quantitative deconvolution of thermal emission spectra," *J. Geophys. Res.*, vol. 103, no. B1, pp. 577–596, Jan. 1998.

[5] A. R. Pratt, N. S. McIntyre, and S. J. Splinter, "Deconvolution of pyritre, marcasite and arsenopyrite XPS spectra using the maximum entropy method," *Surf. Sci.*, vol. 396, pp. 266–272, 1998.

[6] F. W. Wehrli, J. Ma, J. A. Hopkins, and H. K. Song, "Measurement of R_2' in the presence of multiple spectral components using reference spectrum deconvolution," *J. Magn. Res.*, vol. 131, pp. 61–68, 1998.

[7] M. Ben Slima, L. Szczecinski, D. Massicotte, R. Z. Morawski, and A. Barwicz, "Algorithmic specification of a specialized processor for spectrometric applications," *IEEE Trans. Instrum. Meas.*, submitted for publication.

[8] L. Szczecinski, R. Z. Morawski, and A. Barwicz, "Numerical correction of spectrometric data using a rational filter," *J. Chemometr.*, vol. 12, no. 6, pp. 379–395, 1998.

[9] M. Wisniewski, R. Z. Morawski, and A. Barwicz, "Using rational filters for digital correction of a spectrometric micro-transducer," *IEEE Trans. Instrum. Meas.*, vol. 49, pp. 43–48, Feb. 2000.

[10] D. Massicotte, R. Z. Morawski, and A. Barwicz, "Incorporation of a positivity constraint into a kalman-filter-based algorithm for correction of spectrometric data," *IEEE Trans. Instrum. Meas.*, vol. 44, pp. 2–7, Feb. 1995.

[11] M. Ben Slima, R. Z. Morawski, and A. Barwicz, "Kalman-filter-based algorithms of spectrometric data correction—Part II: use of splines for approximation of spectra," *IEEE Trans. Instrum. Meas.*, vol. 46, pp. 685–689, June 1997.

[12] R. Z. Morawski, A. Miekina, and A. Barwicz, "The use of deconvolution and iterative optimization for spectrogram interpretation," *IEEE Trans. Instrum. Meas.*, vol. 46, pp. 1049–1054, Aug. 1997.

[13] B. A. Barsky, *Computer Graphics and Geometric Modeling Using Beta-Splines*. Berlin, Germany: Springer-Verlag, 1988.

Michal P. Wiśniewski was born in 1971 in Poland. He received the M.S. degree in electrical engineering from the Warsaw University of Technology, Warsaw, Poland, in 1995 and the Ph.D. degree in electrical engineering from the University of Quebec, Trois-Rivieres, QC, Canada, in 1999.

Since 1999, he has been with Measurement Microsystems Inc., Trois-Rivieres, and is currently Vice President of Engineering. His research interests are concentrated on the engineering aspects of the monitoring of optical telecommunication channels and applications of digital signal processing in spectrometry, and he has published several technical papers in this area.

Roman Z. Morawski (M'93–SM'98) was born in Poland in 1949. He received the M.S. degree (with honors) in electronic instrumentation from the Warsaw University of Technology, Warsaw, Poland, in 1972, the Ph.D. degree in computing processes and structures from the Leningrad Institute of Electrical Engineering, Leningrad, USSR, in 1979, the higher doctor's degree in measurement applications of digital signal processing from Warsaw University of Technology in 1990, and the Professor's title from the President of the Republic of Poland in 2001.

Since 1972, he has been with the Group on Computer-Assisted Measurements, Institute of Radioelectronics, Faculty of Electronics and Information Technology, Warsaw University of Technology, currently as Professor. He spent four years in Canada from 1988 to 2002 as Visiting Professor at University of Quebec, Trois-Rivieres, QC, and as Senior Research Adviser at Measurement Microsystems Inc. From 1993 to 1999, he was the Senior Associate Dean and, from 1999 to 2002, the Dean of the Faculty of Electronics and Information Technology, Warsaw University of Technology. His research interests are concentrated on the software aspects of measurement. He has published more than 150 papers and two monographs on applications of mathematical modeling and digital signal processing in measurement and instrumentation.

Dr. Morawski is a member of the Polish Society for Measurement, Automatic Control, and Robotics (POLSPAR) and a member of the Committee for Metrology and Instrumentation, Polish Academy of Sciences. He is a member of the American Society for Engineering Education, a Fellow of the Institution of Electrical Engineers (U.K.), and a member of the General Council of International Measurement Confederation IMEKO.

Andrzej Barwicz (M'83) was born in 1942 in Poland. He received the M.S.E.E. and Ph.D. degrees from Warsaw University of Technology, Warsaw, Poland, in 1965 and 1973, respectively.

From 1965 to 1979, he was with the Group of Computer-Assisted Measurements, Warsaw University of Technology. From 1974 to 1979, he was the Head of Postgraduate Study on Computer-Assisted Measurements. From 1979 to 1986, he was an Associate Professor at the Institute of Telecommunications, Oran, Algeria. Since 1987, he has been a Professor with the Department of Electrical Engineering, University of Quebec, Trois-Rivieres, QC, Canada, where he is also Head of the Measuring System Laboratory. Since 1998, he has been Chairman of the Board and CEO of the company Measurement Microsystems, Inc., of which he is also a founder. His professional interests include system approach and measurement microsystems, implemented using microtechnologies and on-chip digital signal processing. He is the author and coauthor of more than 60 technical papers and holds five patents in instrumentation and measurement.

Dr. Barwicz has been involved in the IEEE Instrumentation and Measurement Society activities since 1985. He has served IMTC as author, speaker, session chair, papers reviewer, and conference vice-chair. He is the founder and chair of the Technical Committee on Measurement Microsystems (TC24). He has been an Executive Member of the IEEE St. Maurice Section and, later, Section Chair, and he was IEEE Region 7 Educational Activities Chair from 1996 to 1998.